Topography over South America from ERS Altimetry

Anita Brenner — Hughes STX Corp., 7701 Greenbelt Md. Suite 400 Greenbelt, MD 20770
anita ice.stx.com

Herb Frey — NASA/Goddard Space Flight Center ,Code 921 Greenbelt, MD
frey denali.gsfc.nasa.gov

John DiMarzio, Lucia Tsaoussi — Hughes STX Corp., 7701 Greenbelt Md. Suite 400 Greenbelt, MD 20770
john ice.stx.com , lucia@ice.stx.com

Abstract

The surface topography of South America is mapped from the entire ERS-1 geodetic mission and two 35-day cycles from phase G. The Waveform Altimeter Product from the UK-PAF provides the altimeter waveforms, the range measurement, and the internal and doppler range corrections. We calculate the atmospheric corrections and solid tides, and utilize the University of Delft DGM-E04 precision orbits. Retracking range corrections are calculated using a modified version of the NASA/GSFC waveform retracking algorithm. Our editing scheme removes measurements where the altimeter is hanging onto a specular surface that is not at the subsatellite location. Additional editing is implemented to remove measurements where the tracker has by-passed the closest surface by comparison of the pre-leading edge signal to the overall waveform power. An iterative procedure is used to calculate a 1/4 degree grid from the altimetry, slope correct the altimetry elevations using this grid, and regrid the data. The gridded elevations are then referenced to the NASA/GSFC and NIMA EGM96 geoid. Comparisons of the full-rate altimetry to profiles interpolated from the 1996 ETOPO5 DEM show several instances where altimetry yields detailed topography but the ETOPO5 DEM is smooth due to lack of data. A 1/4 degree grid of the ETOPO5 DEM was created and compared with the altimetric grid. Plots of these grids show whole regions where the altimetry results show topographic features that are smoothed over in the ETOPO5 grid. Comparisons of Shuttle laser altimetry data to the ERS-1 altimetry grid demonstrate agreement in many locations at the sub-meter level. Future plans are to create a more-detailed topographic map combining altimetry from other missions (Geosat geodetic, Seasat, and TOPEX) to increase the resolution of the DEM.

Keywords: Altimetry, Topography, Cartography

Introduction

(Frey and Brenner, 1990) showed that the Seasat over-land measurements could be used, after post-processing of the altimeter waveforms, to measure topography. The Seasat altimeter, however, exhibited many data dropouts and the groundtracks were too sparse for detailed topographic mapping. The Geodetic mission data from Geosat had better geographic coverage, but until recently was classified and is not yet completely available. The ERS-1 altimeter was the first satellite altimeter designed to track over ocean, land, and ice surfaces. Previous altimeters, GEOS-C, Seasat, and Geosat were designed for ocean tracking only.

Two major factors make the ERS-1 altimetry the best available for overland topography. First, the ERS-1 tracker uses a coarser ice tracking mode over the continents that give it the ability to maintain track over the rougher land terrain while only degrading the resolution of the height measurement by a factor of 4 from that in ocean tracking mode. Second, the geodetic portion of the ERS-1 mission consists of two 168-day repeat cycles offset from each other to give a ground-track spacing of 8.5 km at the equator.

Data Processing, Retracking, and Precision

To obtain precise land elevations from ERS-1 satellite altimetry, it is necessary to post-process the altimeter return waveform to correct for tracker misalignment. The UK-PAF's Waveform Analysis Product (WAP), provided through the ESA project, was used as the source of the altimeter range measurement and waveform, the internal range correction, and the doppler range correction. The atmospheric corrections were calculated using the ECMWF data and the University of Texas CSR3.0 tide model (Eanes 1994) was used to model the solid, load and pole tides. The surface elevations were calculated with respect to an ellipsoid of radius 6378137.0 m and a flattening of 1/298.257 using the DGM-E04 orbits (Scharroo *et. al.,* 1996).

The data was retracked using the NASA/GSFC Version 4.0 retracker (Zwally *et. al.,* 1997). The retracking process fits a single-ramp or double ramp (5 or 9-parameter) function to each waveform. The retracker is tuned to pick up distinct ramps and to ignore slight leading edge noise due to vegetation canopy. Altimeter measurements for which the waveform does not have one or two distinct ramps are edited. Analysis of the height residuals at crossing arcs on the corrected, retracked altimetry showed that 9% of the crossing arc differences were greater than 50m. Investigating the waveforms near these crossovers showed two distinct problems; 1) there was excessive signal before the first ramp which may be indicative of the altimeter missing the first return and locking onto a signal from another location, and 2) the altimeter would maintain lock on a specular surface hanging onto the surface even after the satellite moved to another location.

To correct the first problem, the retracking process was modified to edit out returns where the average pre-ramp signal was greater than 20% of the maximum count in any one gate of the whole waveform. This edited out the returns that were truly from a different location, without editing out returns that had a pre-ramp noise due to vegetation canopy. Examples of typical returns over a vegetated region of South America are shown in figure 1 where the raw waveform returns are pictured with the NASA/GSFC Version 4 functional fit and retracking locations for both the functional fit and a 20% threshold retracker. The corresponding altimeter height profile for non-retracked data, threshold retracked data and the functional retracked data is shown in figure 2. Note that the threshold retracking sometimes picks up what the functional fit considers as pre-ramp noise. The threshold retracker may be picking up canopy where the functional-retracked profile appears to follow a more realistic surface. Figure 1 also shows that there is a second distinct spike in the waveforms which increases in amplitude from measurement to measurement. South America is laced with many rivers; these returns indicate there may be a river farther away (around 12 km) that has a more specular return than the subsatellite terrain.

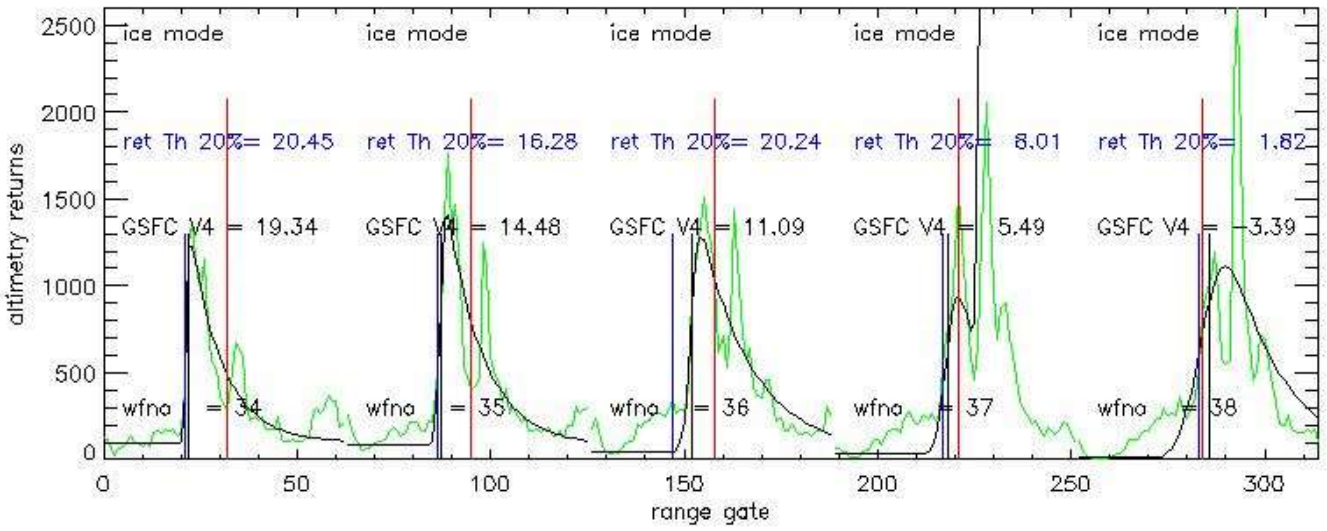

Figure 1: Typical ERS-1 Waveforms over Vegetation.

Waveform numbers refer to elevation profile in Figure 2.

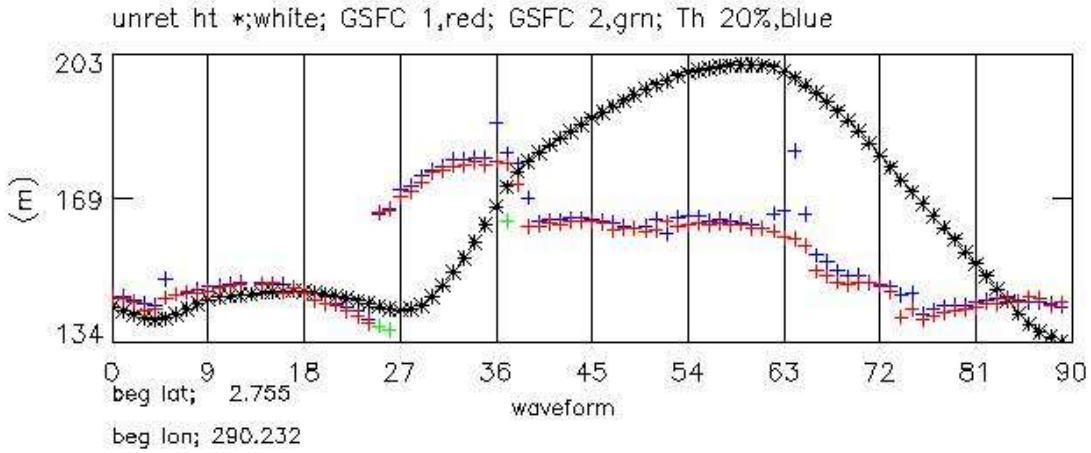

Figure 2: Typical Surface Height Profile

The second problem of hanging onto a specular surface is demonstrated in the altimeter height and automatic gain control, AGC, profiles shown in figures 3a and b. The AGC is a measure of the power in the return. Values of AGC greater than 45 are usually received over very flat deserts, salt flats, rivers or lakes. In figure 3 the retracked surface elevation begins at around 90m elevation with an AGC of 35. The surface elevation sharply decreases to around 75 m as the AGC slowly rises. The surface elevation remains fairly level at around 72 m until waveform 54 where it starts to systematically decrease. During that same period, the AGC has risen into the 50s and stays there until the gradual apparent decrease in surface elevation when the AGC also decreases slowly to the mid 30s. The gradual apparent surface elevation decrease is probably due to the altimeter hanging onto the flat specular surface even after the sub-satellite terrain has changed. At waveform 62 the surface elevation abruptly rises by 25 m and the AGC is in the low 30s. At the very beginning of the elevation rise (waveform 62), there are double-ramp returns where the second ramp is following the initial decreasing profile.

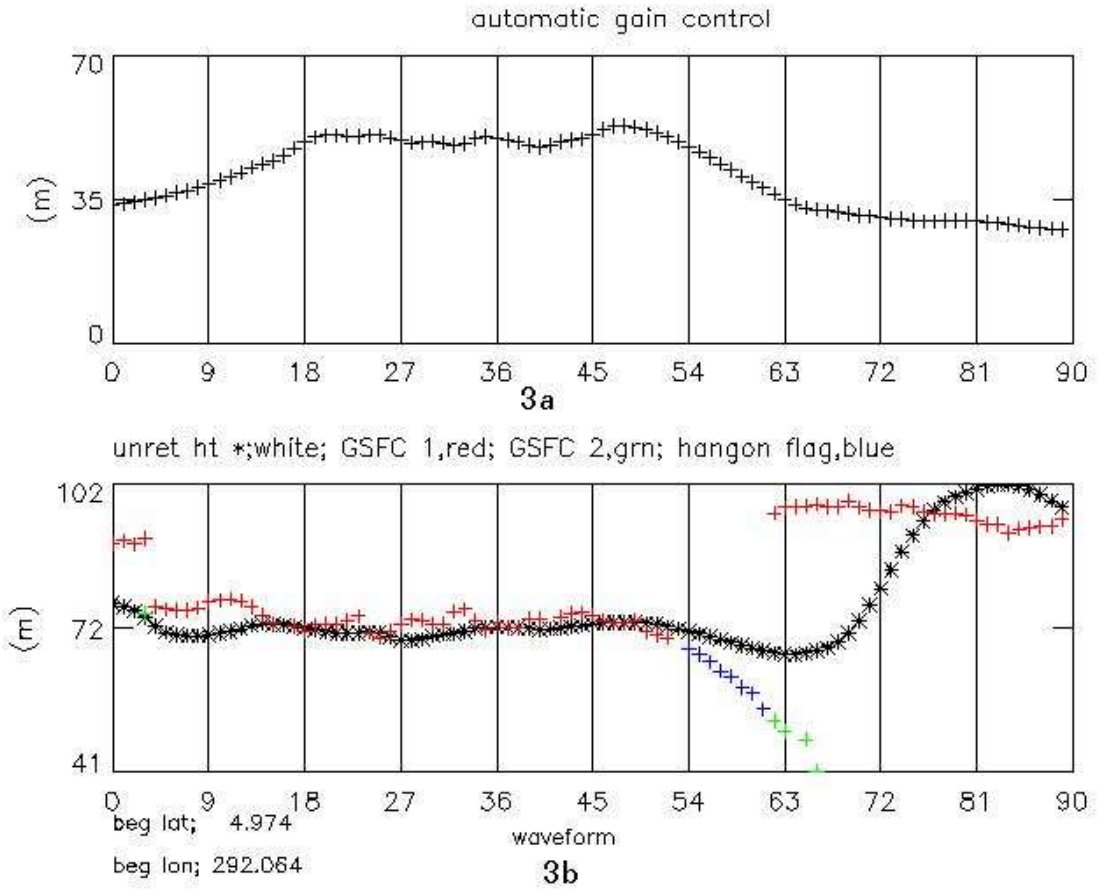

Figure 3: The Altimeter Tracker Hang-on Problem as Illustrated by: a) Automatic Gain Control b) Surface Height Profile

The following steps were used to flag measurements that appeared to be hanging onto a specular surface:

1) A running mean and standard deviation were calculated for all contiguous specular measurements. A measurement was considered specular if the AGC was greater than 45 and the product of the AGC times the maximum gate count was greater than 50,000.

2) If for one second of contiguous data, the standard deviation of (1) above was less than 2.5m then the mean elevation from the preceeding specular data, mnspec, was saved.

3) If contiguous data continued to be specular and the running mean was less than four standard deviations below mnspec then that data was flagged as the beginning of a "hangon segment". All following contiguous data that met the specular criteria in (1) above, and for which the surface elevations were continuously decreasing were flagged as being in the "hangon segment".

All measurements in this "hangon segment" were edited from the final data set. Measurements for waveforms 54 through 61 of figure 3 were edited using this criteria.

The internal precision of the final data set can be measured by calculating the mean and standard deviation of the surface elevation differences for crossing arcs. The mean and standard deviation of these crossovers for all the ERS-1 data used in the calculation of the grid was 15cm and 1.55m respectively.

Gridding and Slope Correction

The altimetric-derived surface elevations were gridded onto an evenly spaced 1/4 degree grid in latitude and longitude. The elevation at each grid node was calculated by taking a weighted average of all data within a given circular region surrounding the node referred to as the cap size. The data was weighted by the inverse of the distance to the grid node. Four different cap size radii were used; 27.75 km, 41.63 km, 55.5km, and 83.25km. The spacing of the altimetry groundtracks over northwest South America with the grid size and different cap sizes is shown in figure 4 for a 5 by 5 degree region of Northwest South America.

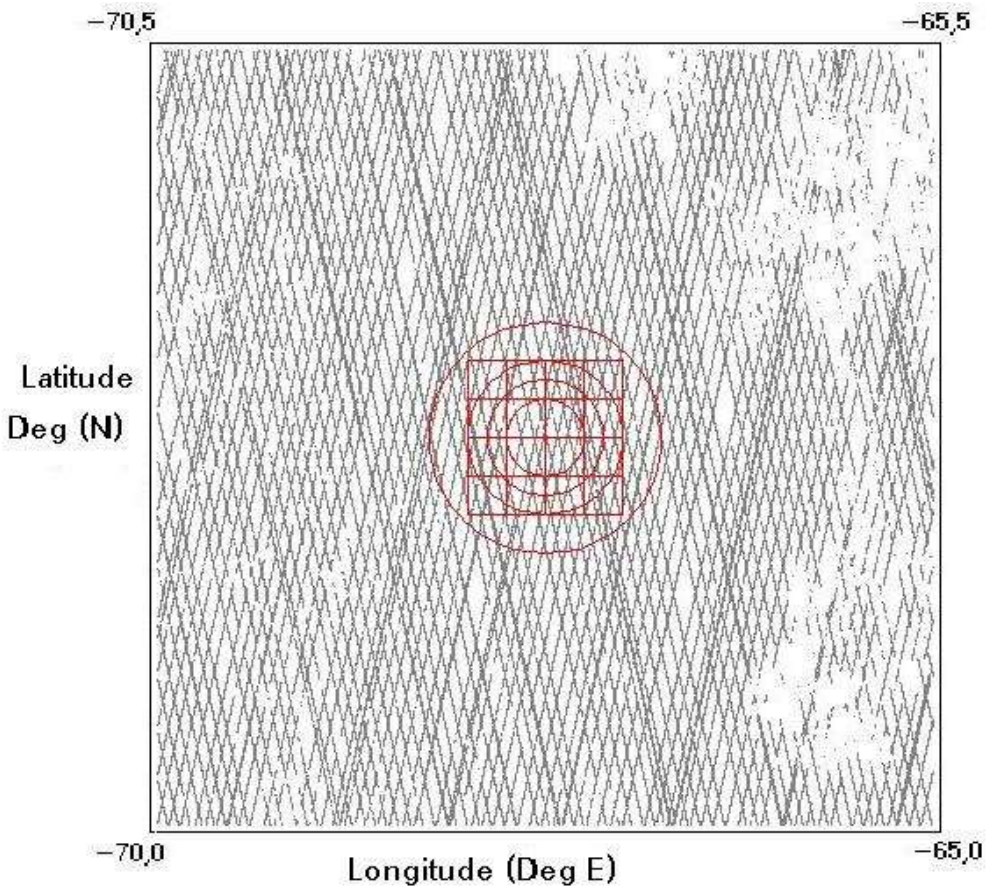

Figure 4: ERS-1 Geodetic Phase Groundtracks with Grid and Cap Sizes

The gridding procedure begins with the smallest cap size and calculates the weighted average. If there are less than 15 elevations or data are not present in at least 3 quadrants of the cap size region, the cap size is increased until these criteria are met. The standard deviation of the data to the weighted average is calculated and data which differ from the gridded elevation by more than 3.5 times this standard deviation are edited. If data are edited, the gridded elevation is recomputed using the remaining data.

This initial grid was used to calculate the slope-induced error for each of the altimeter measurements using the methodology explained in (Brenner *et. al.*, 1983). This error is caused by the altimeter always measuring to the closest surface within the footprint, which over a sloping surface is not the sub-satellite location. For planar-sloping surfaces this error is approximated as

$HTcor_{slope} = H*a^2/2$

where

H = altimeter range measurement
a = the local surface slope

This planar approximation was used to slope correct all the altimeter surface elevations and the data were regridded. The EGM96 geoid (Lemoine *et. al.*, 1996) was subtracted to reference the grid to sea level.

Results

The ERS-1 gridded elevations are shown in figure 5a . The standard deviations of these elevations from the gridding procedure range from under 1 m in the flatter regions to over 200 m in the mountain ranges. The National Imaging and Mapping Association, NIMA, released a new 5 minute DEM in 1996 hereafter referred to as ETOPO5. For most of the continents this included very detailed data. For South America, however, only the data on the northern coast appear updated from the previous ETOPO5 model. We gridded the ETOPO5 data using the same procedure as for the altimetry data for comparison. The ETOPO5 gridded elevations are shown in figure 5b. The same major features are present in both gridded data sets, except the altimetry shows more detail where the ETOPO5 appears to generally smooth out the topography. Differencing the two grids shows a mean difference of -106m with large differences in the mountain ranges where the altimetry is more than 150m lower than the ETOPO5 grid. The altimeter will always measure to the highest elevation in the footprint and the slope correction is an attempt to correct for this. The values of the slope corrections in the mountainous regions range from 5 to 75 m so they cannot account for the large differences we are seeing between the ETOPO5 and altimetry grids.

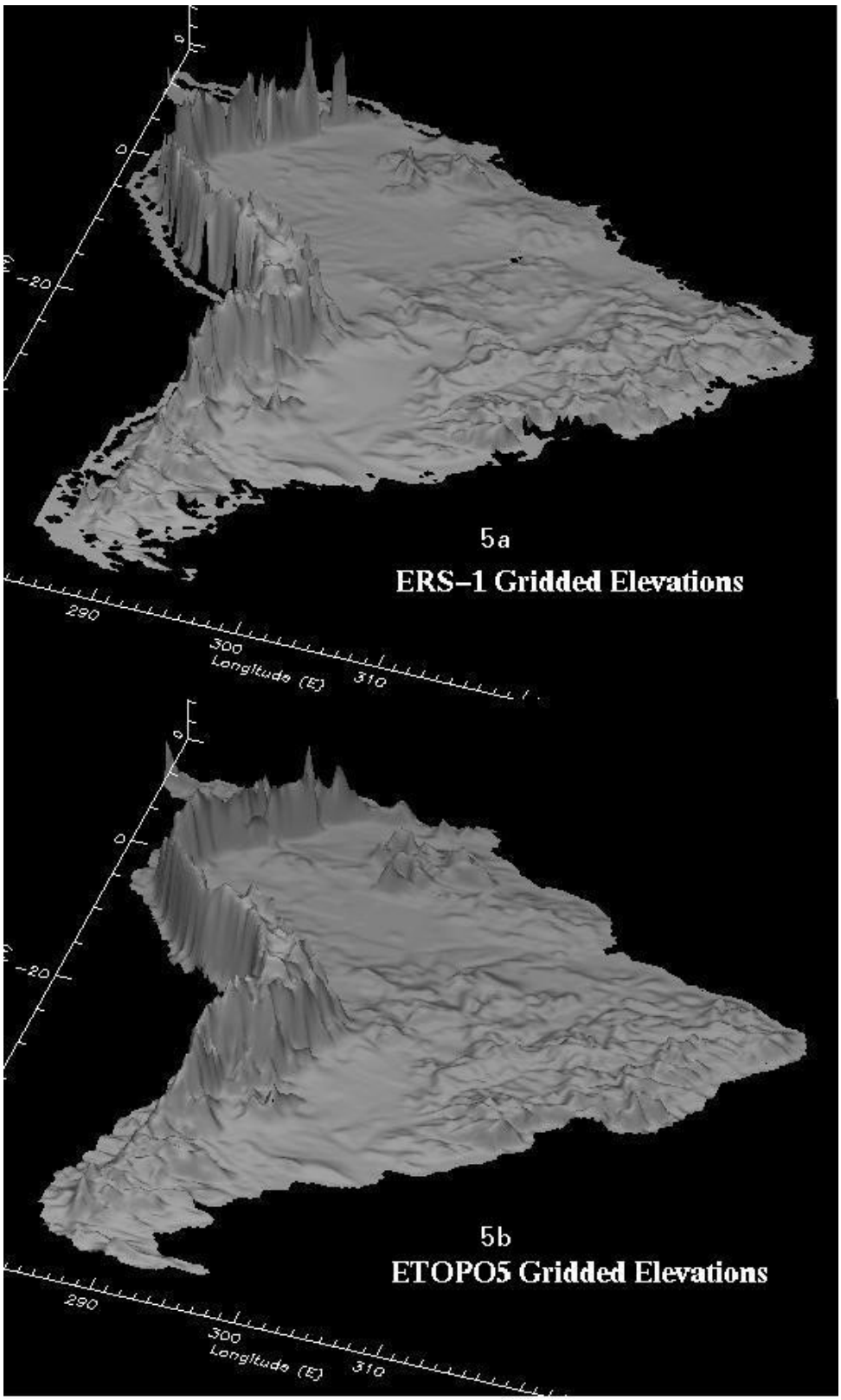

Figure 5: Gridded Elevations from a) ERS-1 Altimetry and b) ETOPO5 DEM

To try to determine how the altimetry differed from the ETOPO5 DEM on a smaller scale, we compared along-track altimetry profiles against a profile interpolated from the full resolution ETOPO5 DEM. A typical example is shown in figure 6 for rev 17793 that runs down the eastern bulge of South America. The altimetry is out of phase with the ETOPO5 DEM data and shows more apparent detail, though it is also noisier. The general trends are similar but the height differences in many locations are more than 100m.

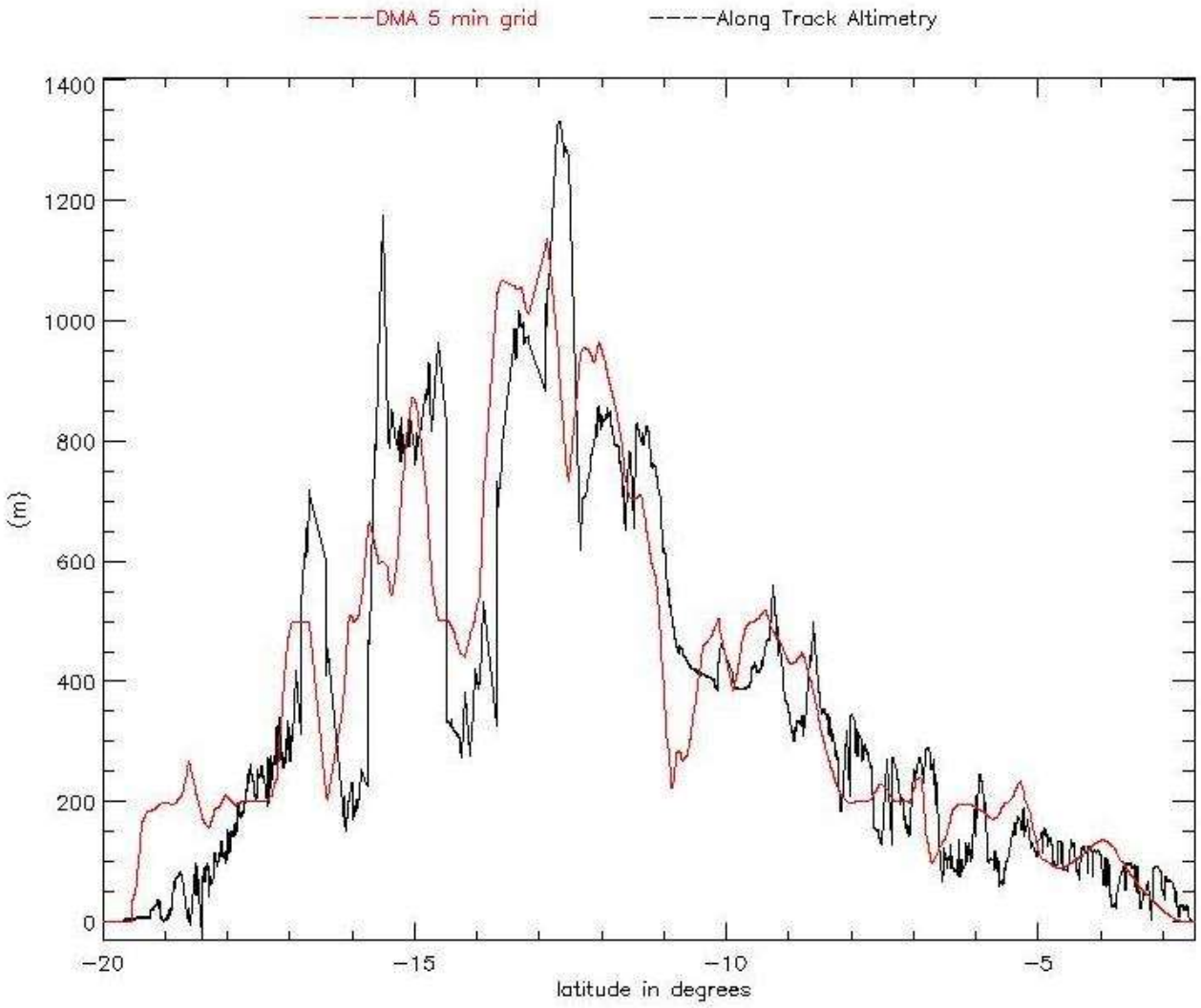

Figure 6: Along-track Altimetry Compared with ETOPO5 5 min DEM

To obtain a quantitative assessment of 1) the accuracy of the ERS-1 grid, 2) the affect of applying the slope correction to the altimetry, and 3) the accuracy of the ETOPO5 grid, we compared all three grids to Shuttle Laser Altimeter, SLA, observations. The SLA has a 100m footprint. The processed elevations over land are believed to be at the 1-2m accuracy level (Garvin *et. al.,* 1997) . We compared the SLA measurements to each of the 3 grids; the slope corrected ERS-1 grid, the non-slope corrected ERS-1 grid, and the ETOPO5 grid by performing a bi-linear interpolation of the grid elevations at the SLA location. Histograms of the differences of the SLA measured elevations minus the grids are shown in figure 7 for all SLA data that agreed to within 100m of each grid respectively. The laser characteristics, the small footprint, and the effect of cloud coverage or canopy height cause many unusable SLA measurements. The 100m cutoff removes any cloud measurements, but the canopy top measurements still remain.

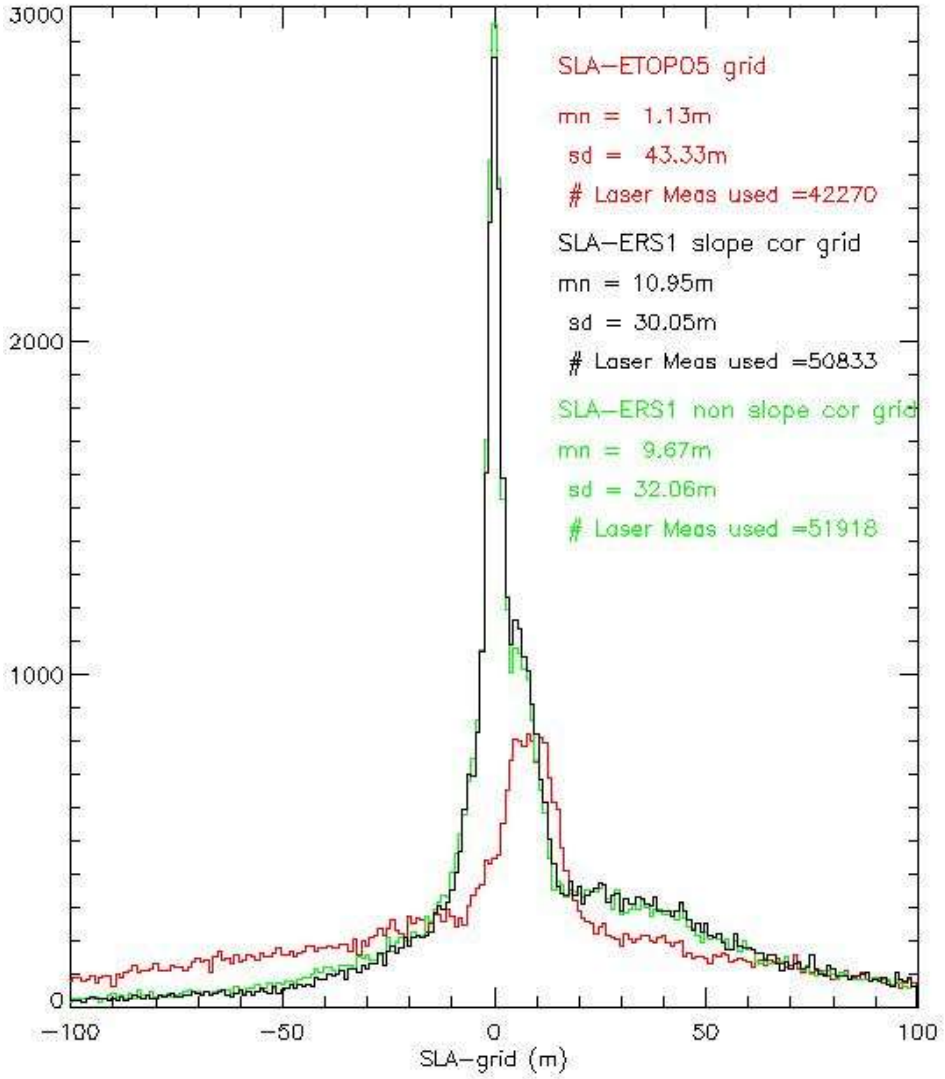

Figure 7: Histograms of Shuttle Laser Altimetry differences with Altimetric and ETOPO5 DEMs

The histograms show that in many locations the SLA data agrees well with the altimetry grids. Over 2500 SLA measurements agree within +/-0.5m and the peak of the histogram is centered at zero. The large amount of differences between 5 and 50 meters are probably due to the laser measuring the vegetation canopy. In contrast, the SLA measurements have much poorer agreement with the ETOPO5 grid where only 500 agree to within 0.5m and the histogram peak is centered at around 10m indicating a general bias in the ETOPO5 grid compared to the SLA.

Figure 8 shows the locations of the SLA data where it agreed to within 1 m of the slope-corrected ERS-1 grid. Note that some of these locations are in regions of rougher terrain though the majority are in the flatter regions.

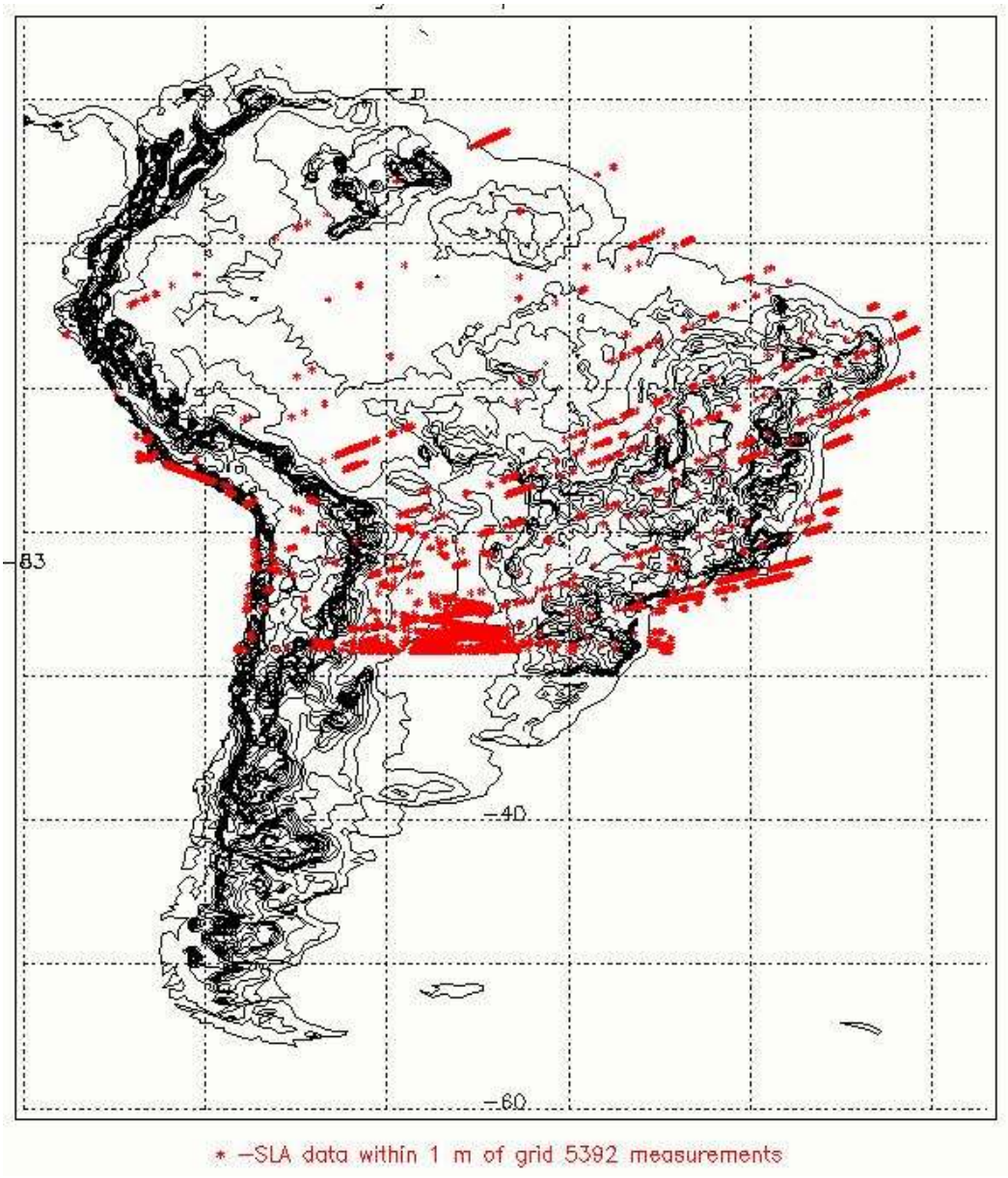

Figure 8: ERS-1 Gridded Heights with respect to the EGM96 Geoid with Locations of SLA data that agree to within 1m

The histograms also show that more of the SLA data agrees to within +/- .5 m of the non-slope-corrected ERS-1 grid than with the slope-corrected grid ERS-1. However the standard deviations of the differences are less with the slope-corrected ERS-1 grid at 30.05m compared to 32.06m for the non-slope-corrected ERS-1 grid. This indicates that the slope correction may be adding error in the regions with low slopes, but in general it is improving the precision of the overall grid.

Conclusions

Satellite radar altimetry data, especially the geodetic phase measurements from ERS-1 can be used to improve on the topographic knowledge of the continents at least for those regions where poor elevation data currently exists such as in South America. The accuracy of the radar altimeter is limited by the large size of the footprint over rougher, mountainous terrain where the errors probably range between 100 and 200 m in contract to the sub-meter accuracy in the plateau regions. However these results show that this data provides a valuable resource for those areas in which the current models lack in detail due to the sparsity of available measurements.

Future plans are to combine altimetry data from Seasat and the geodetic mission of Geosat to increase the resolution of the DEM.

Acknowledgements

This research was supported by NASA's Solid Earth Science Program. We wish to thank Dr. H. Jay Zwally of NASA/Goddard Space Flight Center for the use of his computational resources and Bryan Dixon of Hughes STX Corp. for processing the data.

References

Brenner, A.C., R. A. Bindschadler, R. H. Thomas, and H. J. Zwally, 1983
Slope-Induced Errors in Radar Altimetry Over Continental Ice Sheets. *J. of Geophys. Res.*, Vol. 88, No. C3, pp 1617-1623.

Eanes, R.J., 1994
Diurnal and Semidiurnal Tides from TOPEX/Poseidon Altimetry. *Presented at Spring 1994 AGU Meeting* Baltimore MD.

Frey, H. and A.C. Brenner, 1990
Australian Topography From Seasat Overland Altimetry. *Geophysical Research Letters*, Vol. 17, No. 10, pp 1533-1536.

Garvin, J.B., J.L. Bufton, J.B. Blair, D.J. Harding, S.B. Luthcke, J.A. Marshall, J.J. Frawley, 1997
Observations of the Earth's Topography from the Shuttle Laser Altimeter (SLA): Laser-Pulse Echo-Recovery Measurements of Terrestrial Surfaces and Clouds, *Submitted to Science*.

Lemoine, F.G., *et al.*, 1996
The Development of the NASA GSFC and NIMA Joint Geopotential Model. *Presented at the International Symposium on Gravity, Geoid, and Marine Geodesy* , Tokyo, Japan.

Scharoo R.,P. Visser, and G. Mets, 1997

TOPEX-class Orbits for the ERS Satellites. *Submitted to . of Geophys. Res., ERS Special Section*
Zwally, H.J., A.C. Brenner, J.P. DiMarzio, M. Giovinetto, 1997
Ice Sheet Topography, Slopes, and Flow Directions from ERS Altimetry. *to be presented at the 3rd ERS Symposium* , Florence, Italy.

Keywords: ESA European Space Agency - Agence spatiale europeenne, observation de la terre, earth observation, satellite remote sensing, teledetection, geophysique, altimetrie, radar, chimique atmospherique, geophysics, altimetry, radar, atmospheric chemistry